

Using Gaussian Processes to Design Dynamic Experiments for Black-Box Model Discrimination under Uncertainty

Simon Olofsson¹ · Eduardo S. Schultz² ·
Adel Mhamdi² · Alexander Mitsos² ·
Marc Peter Deisenroth³ · Ruth Misener¹

Received: date / Accepted: date

Abstract Diverse domains of science and engineering use parameterised mechanistic models. Engineers and scientists can often hypothesise several rival models to explain a specific process or phenomenon. Consider a model discrimination setting where we wish to find the best mechanistic, dynamic model candidate and the best model parameter estimates. Typically, several rival mechanistic models can explain the available data, so design of dynamic experiments for model discrimination helps optimally collect additional data by finding experimental settings that maximise model prediction divergence. We argue there are two main approaches in the literature for solving the optimal design problem: (i) the analytical approach, using linear and Gaussian approximations to find closed-form expressions for the design objective, and (ii) the data-driven approach, which often relies on computationally intensive Monte Carlo techniques. Olofsson et al. (ICML 35, 2018) introduced Gaussian process (GP) surrogate models to hybridise the analytical and data-driven approaches, which allowed for computationally efficient design of experiments for discriminating between black-box models. In this study, we demonstrate that we can extend existing methods for optimal design of *dynamic* experiments to incorporate a wider range of problem uncertainty. We also extend the Olofsson et al. (2018) method of using GP surrogate models for discriminating between *dynamic black-box* models. We evaluate our approach on a well-known case study from literature, and explore the consequences of using GP surrogates to approximate gradient-based methods.

Keywords Experimental design · Model discrimination · Gaussian processes

1 Introduction

Mathematical models based on mechanistic assumptions are common in both engineering and the natural sciences, for example pharmaceutical manufactur-

E-mail: simon.olofsson15@alumni.imperial.ac.uk

¹ Department of Computing, Imperial College London, United Kingdom

² Process Systems Engineering (AVT.SVT), RWTH Aachen, Germany

³ Department of Computer Science, University College London, United Kingdom

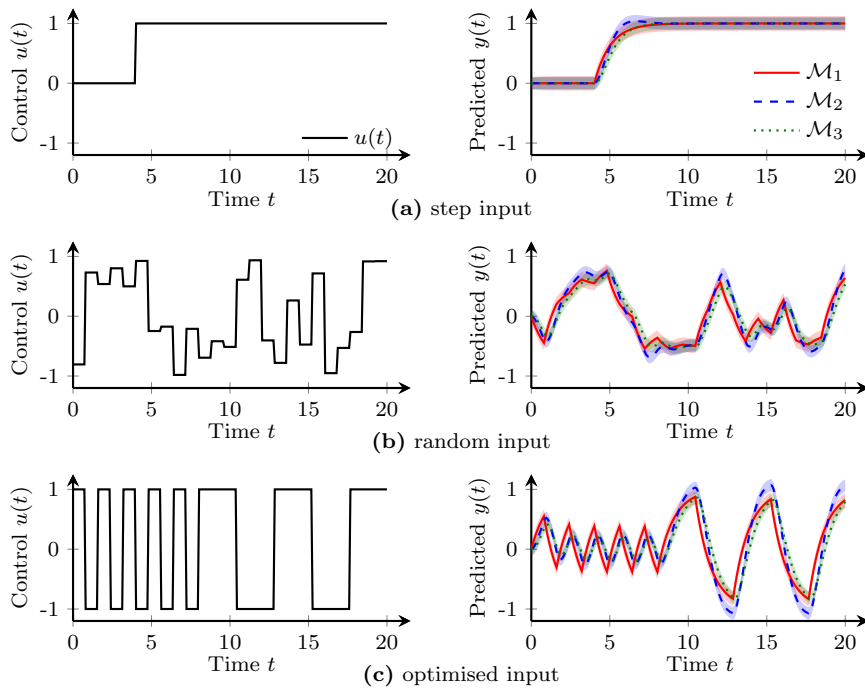


Fig. 1 The three Bania (2019) models \mathcal{M}_1 , \mathcal{M}_2 and \mathcal{M}_3 , defined in Appendix A. The left-hand side show three different piece-wise constant control input as function of time t , and the right-hand side show the corresponding model predictions (mean and two standard deviations).

ing (Chen et al., 2019), climate forecasting (Flato et al., 2014) and high-energy physics (Altarelli, 2014). Researchers and engineers often hypothesise several such mechanistic models to explain the underlying system behaviour. Model discrimination differentiates between these rival hypotheses, i.e. discards inaccurate models (Hunter and Reiner, 1965; Box and Hill, 1967). Often the available experimental data do not allow for discrimination between the rival models, when all models sufficiently explain the available data within data accuracy (Joy et al., 2019). This situation requires running additional experiments to collect more data. But experiments are expensive, so we wish to discriminate between the models with as few additional experiments as possible (Walz et al., 2020).

To illustrate model discrimination, consider three rival, linear continuous-time models \mathcal{M}_1 , \mathcal{M}_2 and \mathcal{M}_3 from Bania (2019). Let $y(t)$ denote the measurement at time t and $u(t)$ the control input. The models account for both process noise and measurement noise. Fig. 1 shows the model predictions for three different piece-wise constant control signals $u(t) \in [-1, 1]$. Fig. 1a shows a step input, and Fig. 1b uniformly distributed random inputs, with the corresponding approximate marginal predictive distributions over time. The different models \mathcal{M}_1 , \mathcal{M}_2 and \mathcal{M}_3 yield different interpretations of underlying system mechanisms. But it is non-trivial to find control inputs yielding sufficiently different predictions to allow for model discrimination.

Observe in Fig. 1a and Fig. 1b that naïvely applying a step or random control input may not produce data resolving the model discrimination problem. A naïve

control input may also result in violations of system safety constraints. Fig. 1c shows an example of a different control signal (developed using the methods presented in this paper). This control signal is optimised to yield sufficiently large model predictions differences for model discrimination. More than one experiment may be required to discriminate between models, and a systematic approach is necessary to minimise the number of experiments.

Another example of a model discrimination scenario comes from Espie and Macchietto (1989) (details in Appendix F). This industrially relevant case study considers four rival models for yeast fermentation, where the controls are the bioreactor inlet velocity and substrate concentration. Yeast fermentation is a very common process in pharmaceutical manufacturing, but the abundance of highly specialised yeast strains (Steensels et al., 2014) make modelling and optimising the processes more difficult.

The examples provided by Bania (2019) and Espie and Macchietto (1989) give easy access to model gradients. But many industrially relevant models, such as those implemented in legacy code, cannot be written in closed form. From an optimisation perspective, these models are effectively black boxes. We can evaluate the models, but the gradients are not readily available. Specialist software can generate the gradients automatically, but this poses substantial requirements on the implementation of the specialist models (Naumann, 2012). For model discrimination, we wish to be agnostic to the software implementation or model type, since this flexibility allows for faster model prototyping and development, and satisfies the personal preferences of researchers and engineers.

In this study, we demonstrate that we can extend existing analytical methods for optimal design of dynamic experiments to incorporate a wider range of problem uncertainty. We also extend the Olofsson et al. (2018) method of using Gaussian process surrogate models, to the case of discriminating between *dynamic* black-box models. We use the well-known case study from Espie and Macchietto (1989) to show that our proposed approach is equivalent to historical approaches when limiting the types of considered uncertainty.

2 Design of Dynamic Experiments for Model Discrimination

We consider state-space formulations of dynamic models (Hangos et al., 2004, Ch. 3). Most of this paper focuses on discrete-time models, but Appendices C and D, respectively, additionally show how to extend our contributions to continuous-time models and discrete-time models with a Δ -transition, which follows from an Euler discretisation of continuous-time dynamics (Atkinson et al., 2009, Ch. 2).

Let $\mathcal{T} = \{t_0, \dots, t_T\}$ denote an ordered set of discrete time instances. These time instances are indexed by $k = 0, \dots, T$, with $k = 0$ the starting time step of an experiment and $k = T$ the final time step. For simplicity, we write $k \in \mathcal{T}$. Assume the system at time step k is in a state $\vec{x}_k = x(t_k) \in \mathbb{R}^{D_x}$. The rate of change of the state is a function of the current state \vec{x}_k , a control input $\vec{u}_k = u(t_k) \in \mathbb{R}^{D_u}$, and some process noise \vec{w}_k . The models describing the rate of change are parameterised by $\vec{\theta} \in \mathbb{R}^{D_\theta}$. The control signal $u(t)$ is commonly discretised and piecewise constant in order to make optimisation feasible in dynamic problems with continuous-time models (Schultz et al., 2019). In general, we cannot observe all

dimensions of the state \vec{x}_k . This is commonly the case for pharmaceutical manufacturing where the models predict different chemical concentrations, only some of which can be measured. Let $\vec{z}_k = z(t_k) \in \mathbb{R}^{D_z}$ denote the observed state. We take measurements $\vec{y}_k \in \mathbb{R}^{D_z}$ of the observed states \vec{z}_k at discrete time instances $k \in \mathcal{T}_{\text{meas}}$. Measurement noise \vec{v}_k corrupts the measurements.

Let $\vec{x}_{0:T}$, $\vec{z}_{1:T}$ and $\vec{u}_{0:T-1}$ denote the sequences of states, observed states and control inputs, respectively. The inputs to the system have dimensionality $T \times D_u + D_\theta$, and the outputs have dimensionality $T \times D_z$. Assume M rival state space models $\mathcal{M}_1, \dots, \mathcal{M}_M$. Model \mathcal{M}_i specifies a state transition, observation and measurement model given a state $\vec{x}_k^{(i)}$, control input \vec{u}_k at time step k , and model parameter vector $\vec{\theta}_i$

$$\mathcal{M}_i : \begin{cases} \vec{x}_k^{(i)} = f_i(\vec{x}_{k-1}^{(i)}, \vec{u}_{k-1}, \vec{\theta}_i) + \vec{w}_{k-1}^{(i)}, & \text{(State transition)} \\ \vec{z}_k^{(i)} = \mathbf{H}_i \vec{x}_k^{(i)}, & \text{(Observed states)} \\ \vec{y}_k^{(i)} = \vec{z}_k^{(i)} + \vec{v}_k^{(i)}, & \text{(Noisy measurement)} \end{cases} \quad (1)$$

where f_i is the transition function, and \mathbf{H}_i is a matrix selecting the observed states. The number of states $D_{x,i}$ may differ between models \mathcal{M}_i , but the number of observed states $D_{z,i} = D_z$ for all models.

We assume the observed state \vec{z}_k is a subset (or linear combination) $\vec{z}_k = \mathbf{H} \vec{x}_k$ of the state. Since the transition function f can be any nonlinear function, this is a minor restriction to the types of models we consider for domains such as pharmaceuticals and chemical manufacturing. Moreover, the methods described in this manuscript could be extended to the more general case of a nonlinear relationship $z(t) = g(x(t))$, where g is known.

The fundamental principle of sequential experimental design for model discrimination says to select the next experimental point where the model predictions differ the most (Hunter and Reiner, 1965). Due to the multiple sources of uncertainty (for example measurement noise) this translates into maximising the divergence between the models' marginal predictive distributions. The problems are, firstly, approximating the models' marginal predictive distributions, and, secondly, constructing and maximising a predictive distribution divergence measure. There are two main approaches to solve these problems: the analytical approach, and the data-driven approach.

The most common analytical approach assumes all uncertainty sources are Gaussian distributed and uses a first-order Taylor expansion around the input mean to propagate the Gaussian input distribution $p(\vec{x}_{k-1}, \vec{u}_{k-1}, \vec{\theta})$ to a Gaussian output distribution $p(\vec{x}_k | \dots)$ (Box and Hill, 1967; MacKay, 1992; Chen and Asprey, 2003). Appendix B offers a more detailed overview. Several closed-form divergence measures exist for Gaussian marginal predictive distributions (Box and Hill, 1967; Buzzi-Ferraris *et al.*, 1990; Michalik *et al.*, 2010; Olofsson *et al.*, 2019). The analytical approach may be computationally efficient, but is also limited in the sense that it requires gradient information and uses linear and Gaussian approximations to handle uncertainty.

The data-driven approach uses Monte Carlo techniques to approximate the marginal predictive distributions' divergence (Ryan *et al.*, 2016). Variational techniques can also be used (Foster *et al.*, 2019). This approach is flexible, because it is agnostic to the model structure (and indifferent to the presence or absence of

function gradients). It may also be more accurate given enough samples, since it does not rely on linearising the models or Gaussian distributed uncertainty. However, it is computationally expensive, does not scale well with the problem size and makes optimisation difficult. As mentioned, the dimensionality of the input and output spaces for the rival models can grow large when we discretise in time. The computational cost associated with solving design of dynamic experiments problems using Monte Carlo techniques would likely become insurmountable. Streif et al. (2014) and Paulson et al. (2019) use polynomial chaos methods for design of dynamic experiments, but must still rely on expensive approximations of the predictive distributions’ divergence. Appendix B offers a more detailed overview.

Olofsson et al. (2018) propose a hybrid approach for black-box model discrimination. They replace the black-box models with Gaussian process (GP) surrogates. GPs are universal function approximators that allow for encoding prior knowledge about the underlying function. Unlike many other surrogate models, GPs also provide prediction uncertainty estimates. Training data for the GP surrogates are collected by evaluating the original black-box model at sampled locations. The GP surrogates are then used in an analytical fashion. This approach is computationally relatively cheap and can accommodate black-box models. However, naïvely applying the Olofsson et al. (2018) approach to design of dynamic experiments is intractable, since it would operate directly on the mapping from $(\vec{x}_0, \vec{u}_{0:T-1}, \mathcal{T}_{\text{meas}})$ to $\vec{z}_{1:T}$. The GP surrogate input dimensionality then scales as $\mathcal{O}(D_x + D_u \times T + D_\theta)$ and output dimensionality as $\mathcal{O}(D_z \times T)$. Even for small T , such as $T = 20$, the dimensionality of the input space is too high for accurate GP inference. The number of GP surrogates would have to equal the output dimensionality, which would be very expensive memory-wise.

Columns (a)–(e) of Table 1 summarise several proposed methods in design of dynamic experiments for model discrimination. This paper extends both the analytical approach of Chen and Asprey (2003) and the Olofsson et al. (2018) GP approach, to design *dynamic* experiments for discriminating black-box models. Column (f) shows the novelty of our proposed approach, for example analytically accommodating black-box models and accounting for all the listed sources of uncertainty. The proposed approach’s GP surrogate input dimensionality scales as $\mathcal{O}(D_x + D_u + D_\theta)$ and output dimensionality as $\mathcal{O}(D_x)$.

2.1 Gaussian Process Regression

A Gaussian process (GP) is a collection of random variables, any finite subset of which is jointly Gaussian distributed. A GP is completely specified by a mean function m and covariance function k (Rasmussen and Williams, 2006). Assume observations $\vec{q} = [q_1, \dots, q_N]^\top$ at locations $\mathbf{R} = [\vec{r}_1, \dots, \vec{r}_N]^\top$, with $q_n \sim \mathcal{N}(g(\vec{r}_n), \sigma_\eta^2)$, of a latent function $g : \mathbb{R}^{D_r} \rightarrow \mathbb{R}$ and zero-mean i.i.d. Gaussian observation noise with variance σ_η^2 . Let ψ denote the GP hyperparameters, which consist of the observation noise variance σ_η^2 and covariance function k ’s parameters. GP regression computes a predictive distribution $g(\vec{r}) | \mathbf{R}, \vec{q}, \psi \sim \mathcal{N}(\mu(\vec{r}_*), \sigma^2(\vec{r}_*))$ at an arbitrary test point \vec{r}_* , with

$$\mu(\vec{r}_*) = m(\vec{r}_*) + \vec{k}^\top (\mathbf{K} + \sigma_\eta^2 \mathbf{I})^{-1} (\vec{q} - \vec{m}), \quad (2a)$$

$$\sigma^2(\vec{r}_*) = k(\vec{r}_*, \vec{r}_*) - \vec{k}^\top (\mathbf{K} + \sigma_\eta^2 \mathbf{I})^{-1} \vec{k}, \quad (2b)$$

Ref.	(a)	(b)	(c)	(d)	(e)	(f)
Nonlinear f	✓	✓		✓	(✓)	✓
Discrete-time models			✓		✓	✓
Continuous-time models	✓	✓		✓		✓
Black-box models				✓		✓
Measurement noise	✓	✓	(✓)	✓	✓	✓
Process noise			✓		✓	✓
Uncertain \vec{x}_0			✓	✓		✓
Uncertain \vec{u}_k						✓
Uncertain $\vec{\theta}$	✓	(✓)		✓		✓
Optimise \vec{x}_0	✓	✓				✓
Optimise $\vec{u}_{0:T-1}$	✓	✓	✓	✓	✓	✓
Optimise $\mathcal{T}_{\text{meas}}$	✓	✓				✓
Path constraints		(✓)	(✓)			✓

Table 1 References: (a) Chen and Asprey (2003), (b) Skanda and Lebedz (2013), (c) Cheong and Manchester (2014), (d) Streif et al. (2014), (e) Bania (2019), (f) This work. Bracketed check marks: Bania (2019) mention how their approach can be extended to non-linear transition functions f ; Cheong and Manchester (2014) has one noise signal that affects both states and measurements; Skanda and Lebedz (2013) use a robust problem formulation instead of marginalising out the model parameters; Skanda and Lebedz (2013) and Cheong and Manchester (2014) solve the design of experiments optimisation problem subject to path constraints that do not account for predicted state uncertainty.

where $[\mathbf{K}]_{j,\ell} = k(\vec{r}_j, \vec{r}_\ell)$, $[\vec{k}]_j = k(\vec{r}_*, \vec{r}_j)$ and $[\vec{m}]_j = m(\vec{r}_j)$. The hyperparameters ψ are typically learnt by maximising the marginal likelihood $p(\vec{g} | \mathbf{R}, \psi)$.

For vector-valued functions (vector fields) $g : \mathbb{R}^{D_r} \rightarrow \mathbb{R}^{D_q}$, we can place independent GP priors $\mathcal{GP}(m_{(d)}, k_{(d)})$ on each target dimension $d = 1, \dots, D_q$, with corresponding covariance function hyperparameters $\psi_{(d)}$. This yields the posterior distribution $g(\vec{r}_*) | \mathbf{R}, \mathbf{Q}, \Psi \sim (M(\vec{r}_*), \Sigma(\vec{r}_*))$, with

$$M(\vec{r}_*) = [\mu_{(1)}(\vec{r}_*), \dots, \mu_{(D_q)}(\vec{r}_*)]^\top, \quad (3a)$$

$$\Sigma(\vec{r}_*) = \text{diag}(\sigma_{(1)}^2(\vec{r}_*), \dots, \sigma_{(D_q)}^2(\vec{r}_*)), \quad (3b)$$

where $\mu_{(d)}(\vec{r}_*)$ and $\sigma_{(d)}^2(\vec{r}_*)$ are the mean and variance given by (2) of the d^{th} GP posterior, $\mathbf{Q} = [\vec{q}_{(1)}, \dots, \vec{q}_{(D_q)}]$, with $\vec{q}_{(d)}$ dimension d of all observations, and $\Psi = \{\psi_{(1)}, \dots, \psi_{(D_q)}\}$ the joint set of hyperparameters. Independent GP priors can accommodate different covariance functions and hyperparameters for different target dimensions.

If the input $\vec{r}_* \sim \mathcal{N}(\vec{\mu}_*, \vec{\Sigma}_*)$ is uncertain, the posterior distribution needs to account for the added uncertainty. The exact posterior distribution is generally intractable but can be approximated, for example with moment matching

$$p(g(\vec{r}_*) | \mathbf{R}, \mathbf{Q}, \Psi, \vec{\mu}_*, \vec{\Sigma}_*) \approx \mathcal{N}(\mathbb{E}_{\vec{r}_*} [M(\vec{r}_*)], \mathbb{E}_{\vec{r}_*} [\Sigma(\vec{r}_*)] + \mathbb{V}_{\vec{r}_*} [M(\vec{r}_*)]). \quad (4)$$

Computing the marginal mean and variance in (4) is also often intractable, with the exception of some special cases (Quiñonero-Candela et al., 2003; Deisenroth et al., 2009). An alternative approximation uses a first-order Taylor expansion of the predictive mean and variance in (2) with respect to \vec{r}_* , and propagates the input distribution through the linearisation $p(g(\vec{r}_*) | \mathbf{R}, \mathbf{Q}, \Psi, \vec{\mu}_*, \vec{\Sigma}_*) \approx$

$\mathcal{N}\left(M(\vec{\mu}_*), \nabla_{\vec{r}}M \vec{\Sigma}_* \nabla_{\vec{r}}M^\top + \Sigma(\vec{\mu}_*)\right)$ where $\nabla_{\vec{r}}M = \partial M(\vec{r})/\partial \vec{r}|_{\vec{r}=\vec{\mu}_*}$. The linearisation is analytically tractable. By construction, the covariance $\nabla_{\vec{r}}M \vec{\Sigma}_* \nabla_{\vec{r}}M^\top + \Sigma(\vec{\mu}_*)$ is positive definite.

3 Experimental Design for Model Discrimination Under Uncertainty

We start from the state-space formulation in (1) to formulate the experimental design optimisation problem for discrimination between rival dynamic models. We aim to demonstrate a single experimental design framework for continuous- and discrete-time models, with analytical or black-box state transition functions. Firstly, we show how we can extend existing methods for design of experiments, particularly that of Chen and Asprey (2003), to include more uncertainty terms, for example in the control input. Secondly, we show how the framework can accommodate GP surrogate models when the transition function is a black box. Thirdly, we outline some best practices (from literature and what we have found useful for GP surrogate models) for handling constraints in our optimisation problem.

In (1), $\vec{w}_k^{(i)}$ is zero-mean Gaussian-distributed process noise and $\vec{v}_k^{(i)} \sim \mathcal{N}(\vec{0}, \vec{\Sigma}_y)$ is independent and identically distributed measurement noise. The process noise $\vec{w}_k^{(i)}$ has known covariance $\vec{\Sigma}_{x,i}$. We assume the measurement noise covariance $\vec{\Sigma}_y$ is known but may be different ($\vec{\Sigma}_y = \vec{\Sigma}_y^{(i)}$) for different models \mathcal{M}_i ¹. Apart from uncertainty due to process noise and measurement noise, we may have uncertainty in the control input, initial state and model parameters.

The control input $\vec{u}_k \sim \mathcal{N}(\hat{\vec{u}}_k, \vec{\Sigma}_{u,k})$ at time step k is Gaussian distributed with mean given by a user-specified desired control input $\hat{\vec{u}}_k$ and covariance $\vec{\Sigma}_{u,k}$. The control covariance $\vec{\Sigma}_{u,k} = \vec{\Sigma}_{u,k}^{(i)}$ may be model-dependent. For simplicity, let the control inputs \vec{u}_k be piece-wise constant and the control covariance constant $\vec{\Sigma}_{u,k} = \vec{\Sigma}_u$. Simple extensions of the framework could accommodate control inputs described e.g. by piece-wise polynomials or time-dependent covariance. Let $\hat{\vec{u}}_{0:T-1} = \{\hat{\vec{u}}_0, \dots, \hat{\vec{u}}_{T-1}\}$ denote the sequence of user-specified control inputs.

The initial state $\vec{x}_0^{(i)} \sim \mathcal{N}(\vec{\mu}_0^{(i)}(\hat{\vec{x}}_0), \vec{\Sigma}_0^{(i)})$ depends on some user-specified initial state settings $\hat{\vec{x}}_0$ common for all models. The vector $\hat{\vec{x}}_0$ is the desired initial state. Model parameters $\vec{\theta}_i \sim \mathcal{N}(\hat{\vec{\theta}}_i, \vec{\Sigma}_{\theta,i})$ are Gaussian distributed with mean given by the maximum *a posteriori* parameter estimate $\hat{\vec{\theta}}_i$. A Laplace approximation computes the model parameter covariance $\vec{\Sigma}_{\theta,i}$ (MacKay, 2003, Ch. 27).

The initial state settings $\hat{\vec{x}}_0$ and the control inputs $\hat{\vec{u}}_{0:T-1}$ determine the experimental outcomes. For continuous-time models \mathcal{M}_i , we may also want to optimise the measurement time points $\mathcal{T}_{\text{meas}}$. Hence, we formulate the optimisation problem of design of dynamic experiments for model discrimination as

$$\arg \max_{\hat{\vec{x}}_0, \hat{\vec{u}}_{0:T-1}} \sum_{k \in \mathcal{T}_{\text{meas}}} D\left(\vec{y}_k^{(1)}, \dots, \vec{y}_k^{(M)}\right) \quad (5a)$$

¹ Note that model-specific measurement noise covariances interferes with some design criterion definitions.

s.t. $\forall k \in \{1, \dots, T\}, \forall i \in \{1, \dots, M\}$:

$$\mathcal{M}_i : \begin{cases} \vec{x}_k^{(i)} = f_i(\vec{x}_{k-1}^{(i)}, \vec{u}_{k-1}, \vec{\theta}_i) + \vec{w}_{k-1}^{(i)}, \\ \vec{z}_k^{(i)} = \mathbf{H}_i \vec{x}_k^{(i)}, \\ \vec{y}_k^{(i)} = \vec{z}_k^{(i)} + \vec{v}_k, \end{cases} \quad (5b)$$

$$\begin{aligned} C_{x_0}(\hat{\vec{x}}_0) \geq \vec{0}, & \quad \left| \quad C_x(\vec{x}_k^{(i)}) \geq \vec{0}, \quad \left| \quad C_{\mathcal{T}}(\mathcal{T}_{\text{meas}}) \geq \vec{0}. \right. \right. \\ C_u(\hat{\vec{u}}_k) \geq \vec{0}, & \quad \left| \quad C_z(\vec{z}_k^{(i)}) \geq \vec{0}, \right. \end{aligned} \quad (5c)$$

$D(\cdot)$ is the design criterion, i.e. a divergence measure between the predictive distributions. C_{x_0}, C_u, C_x, C_z and $C_{\mathcal{T}}$ are constraints on the corresponding variables.

3.1 State Transition

Consider a single model $\mathcal{M} = \mathcal{M}_i$ with corresponding transition operator $\phi = \phi_i$. For a state distribution $\vec{x}_k \sim \mathcal{N}(\vec{\mu}_k, \vec{\Sigma}_k)$, the predicted observed state is $\vec{z}_k \sim \mathcal{N}(\mathbf{H}\vec{\mu}_k, \mathbf{H}\vec{\Sigma}_k\mathbf{H}^\top)$ and the measurement distribution is $\vec{y}_k \sim \mathcal{N}(\mathbf{H}\vec{\mu}_k, \mathbf{H}\vec{\Sigma}_k\mathbf{H}^\top + \vec{\Sigma}_y)$. Solving the optimisation problem in (5) requires the predictive distribution of the latent state \vec{x}_k . This means propagating the uncertainty in the inputs to the transition function f to its outputs. We assume we know *a priori* whether f is an analytical function or a black box, i.e. whether we *do* (analytical) or *do not* (black box) have derivative information of f with respect to its inputs. The derivative information is required for closed-form uncertainty propagation from inputs to outputs using Taylor approximations.

To obtain derivative information from a black-box transition function f , we place independent GP priors $f_{(d)} \sim \mathcal{GP}(m_{(d)}(\cdot), k_{x,(d)}(\cdot, \cdot)k_{u,(d)}(\cdot, \cdot)k_{\theta,(d)}(\cdot, \cdot))$ on output dimensions $d = 1, \dots, D_x$ of f . To simplify notation, let $\mu_f(\cdot) = \mathbb{E}_f[f(\cdot)]$ and $\Sigma_f(\cdot) = \mathbb{V}_f[f(\cdot)]$, such that

$$f(\cdot) \sim \mathcal{N}(\mu_f(\cdot), \Sigma_f(\cdot)) \equiv \begin{cases} \mathcal{N}(f(\cdot), \vec{0}), & f \text{ analytical} \\ \mathcal{N}(\mu(\cdot), \Sigma(\cdot)), & f \text{ black box} \end{cases} \quad (6)$$

where the posterior GP mean $\mu(\cdot)$ and covariance $\Sigma(\cdot)$ are given in (3).

Given an initial state estimate $\vec{x}_0 \sim \mathcal{N}(\vec{\mu}_0, \vec{\Sigma}_0)$, a sequence of control inputs $\vec{u}_k \sim \mathcal{N}(\hat{\vec{u}}_k, \vec{\Sigma}_u)$, $k = 0, \dots, T-1$, a model parameter posterior $\vec{\theta} \sim \mathcal{N}(\hat{\vec{\theta}}, \vec{\Sigma}_\theta)$, and the state transition described by (1), we wish to find the approximate state distribution $\vec{x}_k \sim \mathcal{N}(\vec{\mu}_k, \vec{\Sigma}_k)$ at any time step $k \geq 1$, with mean and covariance given by the moments

$$\vec{\mu}_k = \mathbb{E}_{f, \vec{x}_0, \vec{u}_{0:t-1}, \vec{\theta}, \vec{w}_{0:t-1}} [\vec{x}_k], \quad (7a)$$

$$\vec{\Sigma}_k = \mathbb{V}_{f, \vec{x}_0, \vec{u}_{0:t-1}, \vec{\theta}, \vec{w}_{0:t-1}} [\vec{x}_k]. \quad (7b)$$

Assume that the control covariance $\vec{\Sigma}_u$, model parameter covariance $\vec{\Sigma}_\theta$ and process noise covariance $\vec{\Sigma}_x$ are all constant and independent of \vec{x}_k and $\hat{\vec{u}}_k$.

Let $f(\vec{x}_k) \sim \mathcal{N}(\mu_f(\vec{x}_k), \Sigma_f(\vec{x}_k))$ denote the transition function evaluated at the concatenated state, control input and model parameters $\vec{x}_k = [\vec{x}_k^\top, \vec{u}_k^\top, \vec{\theta}^\top]^\top$, $\vec{x}_k \in \mathbb{R}^{D_x + D_u + D_\theta}$. Assuming the state, control input and model parameters are

Gaussian distributed, the concatenated vector has Gaussian distribution $\tilde{x}_k \sim \mathcal{N}(\tilde{\mu}_k, \tilde{\Sigma}_k)$ with

$$\tilde{\mu}_k = \begin{bmatrix} \tilde{\mu}_k \\ \hat{u}_k \\ \hat{\theta} \end{bmatrix}, \quad \tilde{\Sigma}_k = \begin{bmatrix} \tilde{\Sigma}_k & \vec{0} & \text{cov}(\vec{x}_k, \vec{\theta}) \\ \vec{0} & \tilde{\Sigma}_u & \vec{0} \\ \text{cov}(\vec{x}_k, \vec{\theta})^\top & \vec{0} & \tilde{\Sigma}_\theta \end{bmatrix}, \quad (8)$$

where $\text{cov}(\vec{x}_0, \vec{\theta}) \equiv \vec{0}$, and $\text{cov}(\vec{x}_k, \vec{u}_k) \equiv \vec{0}$ (assuming $\vec{u}_k \neq \vec{u}_{k-1}$) since the latent state cannot depend on future control inputs.

To simplify notation, let $\nabla_{\xi} g$, with $g \in \{f, \mu_f, \Sigma_f, \dots\}$, denote the partial derivative of $g(\xi)$ with respect to a variable ξ , evaluated at the point $\mathbb{E}[\xi]$.

The discrete-time state space model assumes process noise $\vec{w}_k \sim \mathcal{N}(\vec{0}, \tilde{\Sigma}_x)$. Using a first-order Taylor expansion of $\mu_f(\vec{x})$ around $\vec{x}_{k-1} = \tilde{\mu}_{k-1}$, the mean and variance of the latent state at time step $k \geq 1$ in (7a) are approximately given by

$$\begin{aligned} \tilde{\mu}_k &\approx \mu_f(\tilde{\mu}_{k-1}), \\ \tilde{\Sigma}_k &\approx \nabla_{\tilde{x}_{k-1}} \tilde{\mu}_k \tilde{\Sigma}_{k-1} \left(\nabla_{\tilde{x}_{k-1}} \tilde{\mu}_k \right)^\top + \tilde{\Sigma}_x + \Sigma_f(\tilde{\mu}_k), \\ \text{cov}(\vec{x}_k, \vec{\theta}) &\approx \nabla_{\vec{\theta}} \tilde{\mu}_k \text{cov}(\vec{x}_{k-1}, \vec{\theta})^\top + \nabla_{\vec{\theta}} \tilde{\mu}_k \tilde{\Sigma}_\theta. \end{aligned} \quad (9)$$

Note that $\nabla_{\tilde{x}_{k-1}} \tilde{\mu}_k \in \mathbb{R}^{D_x \times (D_x + D_u + D_\theta)}$. We calculate derivatives of $\tilde{\mu}_k$ and $\tilde{\Sigma}_k$ with respect to $\tilde{\mu}_{k-1}$, $\tilde{\Sigma}_{k-1}$ and \hat{u}_{k-1} . The derivatives require second-order derivative information of f or the GP prediction. Appendix C and D have similar expressions to (9) for the latent state transition for continuous-time models and discrete-time models with Δ -transitions, respectively. Appendix E provides an algorithmic description of the design of experiments process.

3.1.1 Combining Original Transition Function and GP Surrogate

The transition function f is replaced with a GP surrogate in (6) to enable analytical approximations of first- and second-order derivatives of f . Equation (6) presents a binary choice between an analytical approach where $\mu_f(\cdot) = f(\cdot)$, and a black-box approach where $\mu_f(\cdot) = \mu(\cdot)$. There is a third possible approach, where the black-box transition function f computes the predictive mean, and the GP surrogate only approximates the derivatives of f . Table 2 compactly shows the difference between the fully analytic approach (where f is analytic), the fully black-box approach (where only the GP surrogate is used) and the proposed third approach (where both f and the GP surrogate are used). The third approach limits the use of the GP surrogates to approximating the gradients of f .

This third approach is appropriate to use during model discrimination, i.e. when analysing agreement between model predictions and experimental observations. This reduces the risk that a model is discarded because of poor accuracy in the GP surrogate prediction. If f is expensive to evaluate, we may still choose to use the GP surrogate black-box approach to speed up the design of experiments in (5). Table 2 shows that for the fully analytic and black-box approaches, the gradient $\nabla \mu_f$ is exact, whereas for the third approach the gradient $\nabla \mu_f(\cdot) \approx \nabla \mu(\cdot)$ is an approximation. This may cause numerical issues when the GP mean $\mu(\cdot)$ —or

Fully analytic approach	Fully black-box approach	Third approach
$\mu_f(\cdot) = f(\cdot),$	$\mu_f(\cdot) = \mu(\cdot),$	$\mu_f(\cdot) = f(\cdot),$
$\Sigma_f(\cdot) = \vec{0},$	$\Sigma_f(\cdot) = \Sigma(\cdot),$	$\Sigma_f(\cdot) = \vec{0},$
$\nabla\mu_f(\cdot) = \nabla f(\cdot)$	$\nabla\mu_f(\cdot) = \nabla\mu(\cdot)$	$\nabla\mu_f(\cdot) \approx \nabla\mu(\cdot)$

Table 2 When f is analytic we use the fully analytic approach in (6). When the transition function f is a black box we may choose to replace it in our computations with a GP surrogate for a fully black-box approach. A third approach is to use the original black-box transition function f for computing $\mu_f(\cdot)$ and the GP surrogate to approximate its gradients $\nabla\mu_f(\cdot)$.

rather the gradient $\nabla\mu(\cdot)$ —does not capture the behaviour in the transition function f with sufficient accuracy. If a numerical solver is provided with inaccurate gradients it may converge slowly to a solution, time-out before reaching any solution, or even throw an error. Therefore, from an optimisation point-of-view, it may be better to use the black-box approach than the third when solving the optimisation problem in (5). On the one hand this means solving an approximation of the optimisation problem, but on the other hand we may be more likely to find a solution.

3.2 Constraints

The optimisation problem in (5) is solved subject to constraints. Constraints are commonly related to safety concerns or physical limitations of the real systems, for example the maximum allowed electrical current in a machine or drug dose given to a patient. However, we may also need to apply constraints on the states $\vec{x}_{1:T}$ if the transition function f is replaced with a data-driven surrogate.

The initial state \hat{x}_0 , the control inputs $\hat{u}_{1:T}$ and the measurement time points $\mathcal{T}_{\text{meas}}$ are independent, deterministic variables, set directly by the user. The states $\vec{x}_{1:T}$ and observed states $\vec{z}_{1:T}$ are dependent, stochastic variables. Constraints on independent and dependent variables are handled differently.

This section considers two types of constraints. Firstly, linear constraints

$$\mathbf{C}\vec{\xi} - \vec{\xi} \geq \vec{0}, \quad (10)$$

where $\vec{\xi} \in \{\hat{x}_0, \hat{u}_k, \vec{x}_k, \vec{z}_k, t_k\}$, $\vec{\xi} \in \mathbb{R}^{D_\xi}$ is an independent or a dependent variable, $\mathbf{C} \in \mathbb{R}^{D_C \times D_\xi}$ and $\vec{\xi} \in \mathbb{R}^{D_C}$, and the inequality is applied element-wise. The constraint may also be time-independent, such that $\mathbf{C}_k = \mathbf{C}$ and $\vec{\xi}_k = \vec{\xi}$, for example for $\vec{\xi} = \hat{x}_0$. The second type of constraints are constraints on the absolute difference, for example the rate of change, between independent variables. We will not consider constraints on the absolute difference between stochastic, dependent variables.

Independent Variable Constraints The independent variables in the optimisation problem in (5) are the initial state settings \hat{x}_0 , the sequence of desired control inputs $\hat{u}_{0:T-1}$ and the measurement time points $\mathcal{T}_{\text{meas}}$ (for continuous-time models). Linear constraints on independent, deterministic variables are straightforward to handle. Note that the constraint in (10) is written in the format of

constraints in the (5) optimisation problem. There may be limitations (for physical or safety reasons) to how quickly the control input \hat{u}_k can be varied. Let the absolute difference in dimension $d = 1, \dots, D_u$ of the control input between consecutive time steps be upper-bounded as $|\hat{u}_{k+1,(d)} - \hat{u}_{k,(d)}| \leq \Delta_{u,(d)}$. Using a standard reformulation, this constraint can equivalently be written as

$$\hat{u}_{k+1,(d)} - \hat{u}_{k,(d)} + \Delta_{u,(d)} \geq 0 \quad \wedge \quad \hat{u}_{k,(d)} - \hat{u}_{k+1,(d)} + \Delta_{u,(d)} \geq 0.$$

Dependent Variable Constraints The dependent variables in the optimisation problem in (5) are the states $\vec{x}_{1:T}$ and observed states $\vec{z}_{1:T}$. Constraints on the dependent variables are typically more difficult to satisfy (Fu et al., 2015), because, as the name suggests, they are dependent on the initial state \vec{x}_0 and the control sequence $\vec{u}_{0:T-1}$.

Let model \mathcal{M} predict the state distribution $\vec{x}_k \sim \mathcal{N}(\vec{\mu}_k, \vec{\Sigma}_k)$ and observed state distribution $\vec{z}_k \sim \mathcal{N}(\vec{\mu}_z, \vec{\Sigma}_z)$ at time step k , where $\vec{\mu}_z = \mathbf{H}\vec{\mu}_k$ and $\vec{\Sigma}_z = \mathbf{H}\vec{\Sigma}_k\mathbf{H}^\top$. Let $\vec{\xi}_k \sim \mathcal{N}(\vec{\mu}_\xi, \vec{\Sigma}_\xi) \in \{\vec{x}_k, \vec{z}_k\}$ denote a Gaussian-distributed dependent variable. To simplify notation, let $\Xi_k \subset \mathbb{R}^{D_\xi}$ denote the space $\Xi_k = \{\vec{\xi} \mid \mathbf{C}_k\vec{\xi} - \vec{\xi}_k \geq 0, \}$ at time step k , such that satisfying the linear constraint in (10) at time k is equivalent to satisfying $\vec{\xi}_k \in \Xi_k$. Multiple sources of uncertainty affect the states $\vec{\xi}_k$ and need to be accounted for. Constraints on dependent variables with unbounded probability distributions (such as Gaussian distributions) are referred to as *chance constraints*. The chance constraint equivalent of $\vec{\xi}_k \in \Xi_k$ is $P(\vec{\xi}_k \in \Xi_k) \geq 1 - \gamma$, for some $\gamma \in (0, 1)$ that determines the chance constraint's confidence level requirement. Chance constraints are typically analytically intractable (Prékopa, 1995, Ch. 11). The range of different tractable approximations for chance constraint include: the scenario approach (Calafiore and Campi, 2006); the sample average approximation (Pagnoncelli et al., 2009); and the convex second-order cone approximation (Mesbah et al., 2014b). This paper only considers the cone approximation, and compares it to a dependent variable constraint that does not account for the uncertainty in the state $\vec{\xi}_k$.

Mean Constraint We let the term *mean constraint* denote the regular linear dependent variable constraint in (10) operating on the state mean, i.e. requiring $\vec{\mu}_\xi \in \Xi_k$. The mean constraint is used by existing literature on design of dynamic experiments (see Table 1). The mean constraint has the advantage of simplicity, at the expense of not accounting for the uncertainty in $\vec{\xi}_k$, and is approximately equivalent to solving the optimisation problem subject to $P(\vec{\xi}_k \in \Xi_k) \geq (\frac{1}{2})^{D_\xi}$. Hence, the mean constraint provides a poor guarantee that the constraint $\vec{\xi}_k \in \Xi_k$ will be satisfied for all time steps k .

Cone Constraint The convex second-order cone approximation (Mesbah et al., 2014b) decomposes the linear dependent variable constraint in (10) into multiple constraints $\vec{c}_{k,(j)}^\top \vec{\xi}_k - \bar{\xi}_{k,(j)} \geq 0$, for $\mathbf{C}_k = [\vec{c}_{k,(1)}, \dots, \vec{c}_{k,(D_C)}]^\top$ and $\vec{\xi}_k = [\bar{\xi}_{k,(1)}, \dots, \bar{\xi}_{k,(D_C)}]^\top$. Each individual chance constraint $P(\vec{c}_{k,(j)}^\top \vec{\xi}_k - \bar{\xi}_{k,(j)} \geq 0) \geq 1 - \gamma$ can be satisfied by

$$\begin{bmatrix} \vec{c}_{k,(j)}^\top \\ \vec{c}_{k,(j)}^\top \end{bmatrix} \vec{\mu}_\xi + \alpha \sqrt{\vec{c}_{k,(j)}^\top \vec{\Sigma}_\xi \vec{c}_{k,(j)}} \begin{bmatrix} 1 \\ -1 \end{bmatrix} - \begin{bmatrix} \bar{\xi}_{k,(j)} \\ \bar{\xi}_{k,(j)} \end{bmatrix} \geq \vec{0},$$

where $\alpha = \sqrt{2} \operatorname{erf}^{-1}(1 - \gamma)$, with $\operatorname{erf}^{-1}(\cdot)$ the inverse error function.

For a fixed covariance $\vec{\Sigma}_\xi$, the cone constraint is equivalent to the mean constraint for a smaller space $\hat{\Xi}_k \subset \Xi_k$. While mean constraint may poorly guarantee satisfying the chance constraint, the cone constraint may be overly conservative since it decomposes the full chance constraint into individual chance constraints.

3.2.1 State Constraints for Data-Driven Surrogate Models

When solving (5), the predicted states $\vec{\mu}_k$ may stray away from the state space region where there is state training data $\mathbf{X} = \{\vec{x}_1, \dots, \vec{x}_N\}$. This can cause numerical issues in the solver as the GP predictive variance grows large, and we may have reasons not to trust a corresponding allegedly optimal solution $\hat{u}_{0:T-1}$. Hence $\vec{\mu}_k$ should be appropriately constrained as $\vec{\mu}_k \in \mathcal{X}$.

Assume we know the feasible control space \mathcal{U} defined by the input constraints. Control input training data can be sampled appropriately to fill \mathcal{U} . We sample model parameter training data in a small region around the maximum *a posteriori* parameter estimate $\hat{\theta}$, to gradient estimation for the Laplace approximation of $\vec{\Sigma}_\theta$. Assume the observed state $\vec{z}_k = \mathbf{H}\vec{x}_k$ is subject to a constraint $\vec{z}_k \in \mathcal{Z}, \forall k \in \mathcal{T}$. We want to sample state training data from a domain $\mathcal{X}^* = \{\vec{x}_k \mid \exists \vec{u}_k \in \mathcal{U} : \mathbf{H}\vec{x}_k \in \mathcal{Z} \iff \mathbf{H}\vec{x}_{k+1} \in \mathcal{Z}\}$, where states \vec{x}_k satisfy $\vec{z}_k \in \mathcal{Z}$ and some control input \vec{u}_k generates an observed state $\vec{z}_{k+1} \in \mathcal{Z}$. Finding \mathcal{X}^* is non-trivial even if the inverse transition function f^{-1} is known. \mathcal{X}^* can be approximated through exhaustive sampling, but this may be expensive. Proceeding, we let $\mathbb{Z}_x = \{1, \dots, D_x\}$ and assume $\mathcal{X}(\vec{x}, \vec{x}) = \{\vec{x} \mid \forall d \in \mathbb{Z}_x : \underline{x}_{(d)} \leq x_{(d)} \leq \bar{x}_{(d)}\} \approx \mathcal{X}^*$ is a known hypercube. GP training data is sampled from \mathcal{X} . We assume state training data is sampled from a grid (with samples on the borders of \mathcal{X}) and combined with control training data and model parameter samples. To maintain a fixed training data density, the training data set has to grow exponentially with state dimensionality D_x and control input dimensionality D_u .

For numerical stability when solving (5), we propose using state constraint $\vec{\mu}_k \in \mathcal{X}(\vec{x} - \vec{\chi}_{d_{\text{out}}}, \vec{x} + \vec{\chi}_{d_{\text{out}}})$ for the GP surrogate corresponding to output dimension d_{out} of f , $d_{\text{out}} \in \mathbb{Z}_x$, where $\chi_{d_{\text{out}},(d)} \equiv |\bar{x}_{(d)} - \underline{x}_{(d)}| / \lambda_{(d_{\text{out}}),(d)}$ and $\lambda_{(d_{\text{out}}),(d)}$ denotes input dimension d 's lengthscale hyperparameter of output dimension d_{out} 's GP surrogate's state covariance function $k_{x,(d)}$. This ensures $\mathcal{X}(\vec{x}, \vec{x}) \subset \mathcal{X}(\vec{x} - \vec{\chi}_{d_{\text{out}}}, \vec{x} + \vec{\chi}_{d_{\text{out}}}), \forall d_{\text{out}} \in \mathbb{Z}_x$.

4 Results

We present computational results for an Espie and Macchietto (1989) case study that considers yeast fermentation. Constants (true parameter values, noise covariances, etc.) are from Chen and Asprey (2003). Yeast fermentation is common in pharmaceutical manufacturing (Martínez et al., 2012). There are $D_x = 2$ states (biomass and substrate concentration) and $D_u = 2$ control inputs. We observe both states, hence $D_z = D_y = 2$ and $\mathbf{H}_i = \mathbf{H} = \mathbf{I}$. The models have $D_{\theta,i} \in \{3, 4\}$ model parameters. Appendix F describes the case study in detail.

Section 4.1 presents a comparison to literature results for the Espie and Macchietto (1989) case study, and Section 4.2 a performance comparison of mean and cone constraints. In Section 4.3 we use simulations to assess the effect of correctly

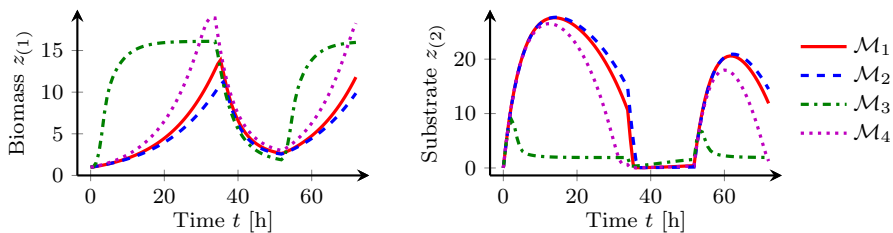


Fig. 2 Predictions by the four models in Espie and Macchietto's (1989) yeast fermentation case study, given optimal control inputs \mathbf{U}_{EM}^* .

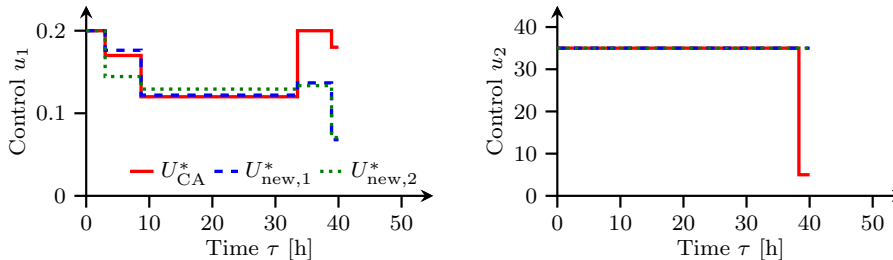


Fig. 3 Optimal control inputs U_{CA}^* from Chen and Asprey (2003), our solution $U_{new,1}^*$, and our solution $U_{new,2}^*$ for the case of added process noise. We see that adding process noise affects the optimal control signal.

modelled, underestimated or overestimated control signal uncertainty, and in Section 4.4 we study the GP surrogate model's performance as analytic emulators of black-box transition functions. We follow the design of experiments process outlined in Algorithm 1 in Appendix E.

4.1 Comparison to Literature

Espie and Macchietto (1989) do not consider any uncertainty in their experimental design algorithm. Let \mathbf{U}_{EM}^* denote the optimal control signal found by Espie and Macchietto (1989). Fig. 2 shows the corresponding model predictions. We use the model parameter values θ_i reported in Espie and Macchietto (1989). If we perturb the elements of \mathbf{U}_{EM}^* by 1.5%, 5% and 10% and use the perturbed inputs as the initial point for the optimisation algorithm, we retrieve \mathbf{U}_{EM}^* again.

Let us add parametric uncertainty and a design criterion accounting for measurement noise. Chen and Asprey (2003) discriminate between the two most similar models: \mathcal{M}_1 and \mathcal{M}_2 . They find 20 optimal measurement time instances \mathcal{T}_{meas} and an optimal control signal U_{CA}^* consisting of 5 piece-wise constant sections. Using the Chen and Asprey (2003) divergence measure, we find objective function value 2601 for their solution. For the same measurement time instances and control switch time instances, we find a solution $U_{new,1}^*$ with objective function value 2805, i.e. a 7.8% larger divergence. Since the problem formulation is identical, we assume this discrepancy is due to the improvement in optimisation solvers after 20 years.

We add process noise with variance $\vec{\Sigma}_x \equiv 0.01 \cdot \mathbf{I}$ (same order of magnitude as the measurement noise). Chen and Asprey’s (2003) optimal control signal U_{CA}^* yields a divergence of 244 with the new (noisier) problem formulation. Fig. 3 shows our solution $U_{\text{new},2}^*$ that yields a divergence of 263, an 8% larger divergence. Fig. 3 shows that $U_{\text{new},1}^* \neq U_{\text{new},2}^*$, which means that adding process noise affects the optimal control signal.

4.2 Comparing Constraints

We compare the results of solving the design of experiments optimisation problem in (5) using either a mean constraint, or a cone chance constraint with $\alpha = 2$ standard deviations margin. We compare the constraints’ performance in terms of the number of constraint violations, how severe the violations are, and the number of experiments required for successful model discrimination. This requires choosing a model discrimination criterion. The model discrimination literature describes several different discrimination criteria (Box and Hill, 1967; Buzzi-Ferraris et al., 1990; Michalik et al., 2010). Following Buzzi-Ferraris et al. (1990), we consider the χ^2 test. The weighted squared residuals $\delta_k^{(i)} = (\vec{y}_k - \mathbf{H}_i \vec{\mu}_k^{(i)})^\top (\mathbf{H}_i \vec{\Sigma}_k^{(i)} \mathbf{H}_i^\top + \vec{\Sigma}_y)^{-1} (\vec{y}_k - \mathbf{H}_i \vec{\mu}_k^{(i)})$ should be χ^2 -distributed. The χ^2 score is 1 minus the χ^2 cumulative distribution at $\sum_{k \in \mathcal{T}_{\text{meas}}} \delta_k^{(i)}$ with $|\mathcal{T}_{\text{meas}}| \times D_y - D_{\theta,i}$ degrees of freedom. Models are inadequate if their χ^2 score is below some threshold, such as 1E-3.

Let \bar{z}_2 be a constraint upper bound on the substrate concentration, such that we wish to satisfy $z_{k,(2)} \leq \bar{z}_2$ for $k = \{1, \dots, T\}$. For the simulations, the upper bound takes a value $\bar{z}_2 \in \{7, 10, 15\}$. Measurements $\vec{y}_{1:T}$ are generated in each simulated experiment and used for model discrimination, with models deemed inadequate if their χ^2 score is below 1E-3. Table 3 shows the performance in 25 simulations of the different state constraint types (mean constraint and cone constraint) in terms of the average number of experiments needed for successful model discrimination; All simulations correctly identify Model \mathcal{M}_1 as the true data-generating model. At least for the test instance by Chen and Asprey (2003), the additional conservatism of the cone constraints does not lead to more required experiments or better model prediction performance.

But the following results indicate that the conservatism of the cone constraints do indeed increase the safety of the control signal by lowering the violation. We generate the experimental measurements $\vec{y}_{1:T}$ from one particular realisation of initial state, control inputs and measurement noise. If the constraints are not violated for this particular noise realisation, they may still be violated for other experiments generated using the same optimal control signal $\hat{u}_{1:T}^*$. Therefore, we use Monte Carlo sampling to better assess the safety of a control signal.

We generate data by evaluating model \mathcal{M}_1 , with “true” model parameter values $\vec{\theta}^{(0)}$ from Chen and Asprey (2003). Let \mathcal{M}_0 denote the data-generating model, with transition function $f_0(\cdot, \cdot) = f_1(\cdot, \cdot, \vec{\theta}^{(0)})$. Assume we are studying an optimised control sequence $\hat{u}_{0:T-1}^*$. We generate a large number $N_{\text{sim}} = 100$ of noisy control sequences $\vec{u}_{0:T-1,n}$, $n = 1, \dots, N_{\text{sim}}$ by drawing samples $\vec{u}_{k,n} \sim \mathcal{N}(\hat{u}_k^*, \vec{\Sigma}_u)$. For each control sequence, we sample a random initial state $\vec{x}_{0,n} \sim \mathcal{N}([1, 0.01]^\top, \vec{\Sigma}_0)$ and process noise sequence $\vec{w}_{0:T-1,n}$. The control sequences, initial states and process noise sequences are used with \mathcal{M}_0 to generate corresponding sequences of

Bound	Constraint	Experiments required		Avg. num. of models remaining after #n exp.		
		Mean	Std	#1	#2	#3
7	Mean	2.02	0.14	2.00	1.02	1
	Cone	2.42	0.50	2.54	1.42	1
10	Mean	2.04	0.20	2.00	1.04	1
	Cone	2.16	0.37	2.16	1.16	1
15	Mean	2.12	0.33	2.02	1.12	1
	Cone	2.02	0.14	2.02	1.02	1
15	Cone	2.12	0.33	2.08	1.12	1

Table 3 Average number of experiments required (with standard deviation) to discard the incorrect models in 25 simulations of the yeast fermentation case study, with a mean or cone constraint (Section 3.2) with an upper bound on $z_{k,2}$. The right-most columns show the average number of models (out of four) that pass the χ^2 test after 1, 2 or 3 experiments. The last row shows the result for the GP surrogate approach in Section 4.4. For the test instance by Chen and Asprey (2003), the additional conservatism of the cone constraints does not lead to more required experiments or better model prediction performance.

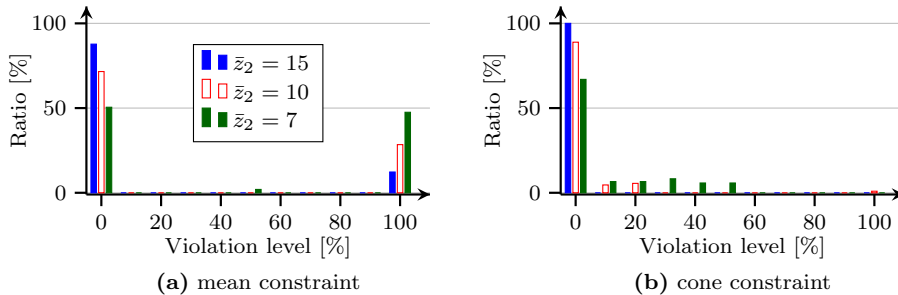


Fig. 4 The violation level is the ratio of Monte Carlo simulations using optimised control signals that result in constraint violations $z_{k,(2)} > \bar{z}_2$. The vertical axes show the ratio of optimised control signals for each violation level (horizontal axes) for a given constraint.

observed states $\bar{z}_{1:T,n}$. Let $\mathbf{Z} = \{\bar{z}_{1:T,1}, \dots, \bar{z}_{1:T,N_{\text{sim}}}\}$ denote the set of observed state sequences. Next, let $\mathbf{Z}_{\text{viol}} = \{\bar{z}_{1:T} \mid \bar{z}_{1:T} \in \mathbf{Z} \wedge \exists k : z_{k,(2)} > \bar{z}_2\}$ be the set of observation sequences for which the constraint $z_{k,(2)} \leq \bar{z}_2$ is violated for at least one time step k . The experiment *violation level* is the relative size $|\mathbf{Z}_{\text{viol}}|/N_{\text{sim}}$. A violation level of 0% means that a given control signal is apparently safe, while a violation level of 100% means that a control signal is almost guaranteed to result in constraint violations.

Fig. 4 shows the ratio of experiments, i.e. optimised control signals, at each violation level. Note: The cone constraint results in *fewer* constraint violations than the mean constraint; The cone constraint results in *less severe* constraint violations than the mean constraint; The number of constraint violations increases as the upper bound shrinks. These observations are in line with expectations.

Control covariance		Experiments required		Model discrimination			Cone constraint
$\hat{\Sigma}_u$	$\vec{\Sigma}_u$	Mean	Std	Succ.	Fail.	Inconcl.	violations
small	small	2.04	0.20	100 %	0 %	0 %	0 %
small	large	2.05	0.22	84 %	0 %	16 %	4 %
large	small	2.58	0.97	96 %	0 %	4 %	0 %
large	large	2.21	0.66	96 %	0 %	4 %	0 %

Table 4 The first set of columns shows the modelled control covariance $\hat{\Sigma}_u$ and the true control covariance $\vec{\Sigma}_u$ used for generating experimental data, with $\vec{\Sigma}_{\text{small}} = \text{diag}(1\text{E-}8, 1\text{E-}4)$ and $\vec{\Sigma}_{\text{large}} = \text{diag}(1\text{E-}4, 1\text{E-}2)$. The second set of columns shows the average number of experiments required for successful model discrimination in 25 yeast fermentation case study simulations. The third set of columns shows the ratio of successful, failed or inconclusive model discrimination. The last column shows the ratio of simulations with cone constraint violations.

4.3 Effect of Control Input Uncertainty

Problem (5) assumes several covariance matrices are known. In many applications, the exact covariances are unknown and have to be approximated. We study the effect of under- or overestimating the covariance size by varying the control input covariance $\vec{\Sigma}_u$. More specifically, let the models \mathcal{M}_i assume the control input $\vec{u}_k \sim \mathcal{N}(\hat{u}_k, \vec{\Sigma}_u)$. We generate experimental data by evaluating \mathcal{M}_0 (same as in Section 4.2), using control inputs $\vec{u}_k \sim \mathcal{N}(\hat{u}_k, \vec{\Sigma}_u)$. The *modelled* covariance $\hat{\Sigma}_u$ and the *true* covariance $\vec{\Sigma}_u$ take values $\vec{\Sigma}_{\text{small}} = \text{diag}(1\text{E-}8, 1\text{E-}4)$ or $\vec{\Sigma}_{\text{large}} = \text{diag}(1\text{E-}4, 1\text{E-}2)$. There are four combinations of small and large modelled and true control covariances. The resulting scenarios can be described as (i) correctly modelled uncertainty $|\hat{\Sigma}_u| = |\vec{\Sigma}_u|$, (ii) underestimated uncertainty $|\hat{\Sigma}_u| \leq |\vec{\Sigma}_u|$, and (iii) overestimated uncertainty $|\hat{\Sigma}_u| \geq |\vec{\Sigma}_u|$.

Table 4 shows the result of 25 simulations of the yeast fermentation case study with the different modelled and true control covariances. A cone constraint is enforced with an upper bound $\bar{z}_2 = 15$ (see Section 4.2). As expected, a correctly modelled small control covariance yields the best result in terms of average number of experiments required and the model discrimination success rate. A large modelled control covariance increases the average number of required experiments, and decreases the success rate. Model discrimination *fails* if an incorrect model is identified as the data-generating model, and is *inconclusive* if the experimental budget (maximum number of allowed experiments) is exhausted or the χ^2 -test discards all models as inadequate. These simulations never exhausted the experimental budget, i.e. all inconclusive model discrimination instances are due to all models being deemed inadequate. The rate of inconclusive model discrimination is significantly higher when the true control covariance is underestimated, and we have a cone constraint violation. Hence, we are punished less for conservative estimates of the control covariance than for overly optimistic estimates.

4.4 Black-Box Transition Functions

The next level of difficulty is black-box transition functions. To solve the design of experiments problem with black-box transition functions we introduce our GP sur-

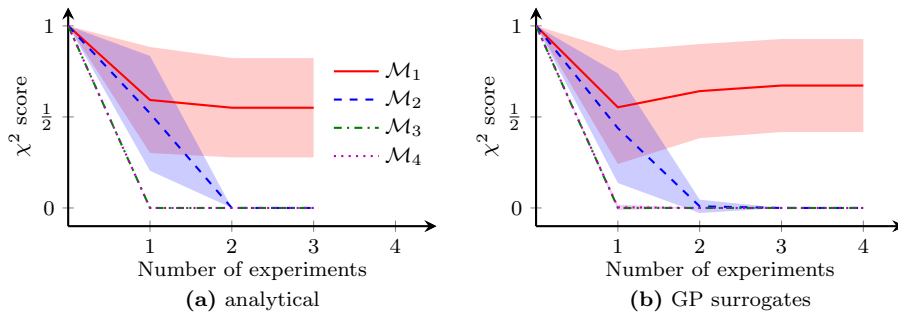


Fig. 5 Evolution of the average χ^2 scores (with one standard deviation) for the four rival models in the yeast fermentation case study, with experiments design using (a) the analytical approach, and (b) the GP surrogates approach.

rogate models. Here we encounter an issue with the model parameter prior covariances. Each simulation starts with no initial data and relatively uninformed model parameter priors. In the Section 4.2 state constraint test and the Section 4.3 control uncertainty test, with analytical transition functions, we use the Appendix F model parameter prior covariance $\bar{\Sigma}_{\theta,i,0} = 0.05 \cdot \mathbf{I}$. However, for the GP surrogates, which additionally incorporate model prediction uncertainty, this covariance is too large and the models' predictive distributions cannot satisfy the constraint $\bar{z}_2 = 15$ with sufficient probability. We solve this by reducing the model parameter prior covariance to $\bar{\Sigma}_{\theta,i,0} = 1\text{E-}4 \cdot \mathbf{I}$ for the GP surrogates. On the one hand, this means the parameter prior may be overly confident with increased risk of constraint violations in the GP surrogate tests. But the optimisation is more likely to converge on a feasible first experiment in each simulation.

We compare the GP surrogate approach to the Section 4.2 analytic results. The last row of Table 3 shows the GP's performance in terms of average number of experiments required for successful model discrimination in 25 simulations of the yeast fermentation case study. Model \mathcal{M}_1 was correctly identified as the true data-generating model in all simulations. The GP surrogate approach has a marginally worse performance than the analytical method. This is expected since the GP surrogate approach emulates the analytical method, but with more uncertain predictions due to the added covariance term in (9). Fig. 5 shows the average χ^2 score evolution (with one standard deviation) for the four rival models in the yeast fermentation case study: Fig. 5a for the analytical approach with a cone constraint, and Fig. 5b using the GP surrogates approach. This illustrates the GP surrogates' marginally worse performance compared to the analytical method. Black-box models yield larger marginal model prediction uncertainty that results in higher χ^2 scores, which means, compared to non-black-box models, more experiments may be required for model discrimination.

5 Discussion

Our work assumes that the black-box model component is the state transition function f . Our problem formulation writes all models as first-order models, i.e. for discrete-time models the state \bar{x}_{k+1} depends only on the state \bar{x}_k , and for

continuous-time models the first-order ordinary differential equation system have only the zeroth-order states $x(t)$ on the right-hand side. All n th order models can be expressed as first-order models by introducing additional states. We also assume the observed states \vec{z}_k are a linear combination of the states \vec{x}_k . Since the transition function f can be any non-linear function, using $\vec{z}_k = \mathbf{H}\vec{x}_k$ is only a minor restriction. State space models are also used in settings where the mapping from state to observed state is highly non-linear, such as in pixels-to-torque problems (Wahlström *et al.*, 2015). Approximate moment matching can infer the predictive distribution for \vec{z}_k for this more general case $\vec{z}_k = g(\vec{x}_k)$.

A limitation of the analytical approach is the use of linear and Gaussian approximations for uncertainty propagation. This is done for analytical (and hence computational) tractability. It is important to be aware that linear approximation and GP surrogates introduce an error at each modelled time step, which may accumulate and grow significantly over longer time horizons. This may lead to poor model predictions, lower-than-expected experimental data informativeness, and constraint violations.

We assume the noise covariances $\vec{\Sigma}_x$ and $\vec{\Sigma}_y$ are known. In practice, estimating these covariances requires domain expertise. Our results in Section 4.3 show that conservative noise covariance estimates produce better results: The model noise covariances should provide reasonable upper bounds to the true noise variance.

Olofsson *et al.* (2018) use GP surrogate models for the mapping from inputs to observed output. With this paper’s notation, this corresponds to the mapping $\vec{x}_0, \vec{u}_{0:T-1}, \vec{\theta} \mapsto \vec{z}_{1:T}$, with input dimensionality $D_x + D_u \times T + D_\theta$ and output dimensionality $D_z \times T$. This approach would not work for design of *dynamic* experiments since the input dimensionality would be too high for accurate GP inference and the output dimensionality (the number of GP surrogate models) would depend on T . We put the GP prior on the state transition, corresponding to the mapping $\vec{x}_k, \vec{u}_k, \vec{\theta} \mapsto \vec{x}_{k+1}$. This gives input dimensionality $D_x + D_u + D_\theta$ and output dimensionality D_x .

We consider an open-loop (offline) control approach, where a designed experiment runs to completion before data is analysed. Galvanin *et al.* (2009) and De-Luca *et al.* (2016) consider a closed-loop (online) approach for parameter estimation. A closed-loop approach repeatedly solves the problem in (5). Although theoretically possible for designing dynamic experiments for model discrimination, the computational cost of our approach would likely be too high in practice.

6 Conclusions

Model discrimination finds mechanistic models that adequately describe and predict a system’s behaviour. Mechanistic models are often needed in industry, for example to satisfy regulatory requirements. We considered a wide range of problem uncertainty, extended traditional analytic approaches for design of dynamic experiments using the Olofsson *et al.* (2018) methodology of replacing black-box models with GP surrogates, and unified the literature contributions for discrete- and continuous-time models. Literature comparisons show that our method reduces to previously acquired results. Both this paper and Olofsson *et al.* (2018) present the GP surrogate approach as hybridising analytical and data-driven experimental design approaches. Condensing the range of possibilities, the GP sur-

rogate approach is closer to the analytical than the fully data-driven approach. But we imagine a spectrum of different trade-offs between accuracy and computational complexity. The posteriors of more advanced GP models may not have closed form expressions (Salimbeni and Deisenroth, 2017), so we may require sampling to approximate the predictive distributions. Hybrid design of experiments approaches using such advanced GP surrogates therefore lie closer to the data-driven approaches. An alternative, hybrid approach could combine mechanistic modelling and data-driven learning for data-driven models with physically meaningful embeddings (Sæmundsson et al., 2020). The model discrimination challenge becomes discerning the effect of the mechanistic versus the data-driven model part.

Author contributions Conceptualisation, S.O. and R.M.; Methodology / Software, S.O. and E.S.S.; Validation / Formal Analysis / Investigation / Data Curation, S.O.; Writing (Original Draft Preparation) / Visualisation, S.O.; Writing (Review and Editing), all; Supervision, Ad.M., Al.M, M.P.D. and R.M.; Project Administration / Funding Acquisition / Resources, Al.M. and R.M.

Funding This work has received funding from the European Union’s Horizon 2020 research and innovation programme under the Marie Skłodowska-Curie grant agreement no. 675251, an EPSRC Research Fellowship (EP/P016871/1), and the Imperial Data Science Institute.

Code availability We generated all results using our open-source Python package for design of experiments, *doepy* (<https://github.com/scwolof/doepy>).

Conflict of interest The authors declare that they have no conflict of interest.

Ethics approval / Consent to participate / Consent for publication Not applicable.

References

- G. Altarelli. The Higgs and the excessive success of the Standard Model. *arXiv:1407.2122*, 2014.
- K. Atkinson, W. Han, and D. Stewart. *Numerical Solution of Ordinary Differential Equations*. John Wiley & Sons, Inc., 2009.
- P. Bania. Bayesian input design for linear dynamical model discrimination. *Entropy*, 21(4):351, 2019.
- G. E. P. Box and W. J. Hill. Discrimination among mechanistic models. *Technometrics*, 9(1):57–71, 1967.
- G. Buzzi-Ferraris, P. Forzatti, and P. Canu. An improved version of a sequential design criterion for discriminating among rival multiresponse models. *Chem Eng Sci*, 45(2):477–481, 1990.
- G. C. Calafiore and M. C. Campi. The scenario approach to robust control design. *IEEE Trans Autom Control*, 51(5):742–753, 2006.
- B. H. Chen and S. P. Asprey. On the design of optimally informative dynamic experiments for model discrimination in multiresponse nonlinear situations. *Ind Eng Chem Res*, 42(7):1379–1390, 2003.
- W. Chen, L. T. Biegler, and S. García Muñoz. A unified framework for kinetic parameter estimation based on spectroscopic data with or without unwanted contributions. *Ind Eng Chem Res*, 58(30):13651–13663, 2019.
- S. Cheong and I. R. Manchester. Input design for model discrimination and fault detection via convex relaxation. In *ACC*, pages 684–690, 2014.
- R. De-Luca, F. Galvanin, and F. Bezzo. A methodology for direct exploitation of available information in the online model-based redesign of experiments. *Comp Chem Eng*, 91:195–205, 2016.
- M. P. Deisenroth and C. E. Rasmussen. PILCO: A model-based and data-efficient approach to policy search. In *ICML 28*, pages 465–472, 2011.
- M. P. Deisenroth, M. F. Huber, and U. D. Hanebeck. Analytic moment-based Gaussian process filtering. In *ICML 26*, pages 225–232, 2009.
- D. Espie and S. Macchietto. The optimal design of dynamic experiments. *AIChE Journal*, 35(2):223–229, 1989.

- G. Flato, J. Marotzke, B. Abiodun, et al. Evaluation of climate models. In *Climate Change 2013: The Physical Science Basis*, pages 741–866. Cambridge University Press, 2014.
- A. Foster, M. Jankowiak, E. Bingham, et al. Variational Bayesian optimal experimental design. In *NeurIPS 32*, pages 14036–14047, 2019.
- J. Fu, J. M. M. Faust, B. Chachuat, et al. Local optimization of dynamic programs with guaranteed satisfaction of path constraints. *Automatica*, 62:184–192, 2015.
- F. Galvanin, M. Barolo, and F. Bezzo. Online model-based redesign of experiments for parameter estimation in dynamic systems. *Ind Eng Chem Res*, 48(9):4415–4427, 2009.
- K. M. Hangos, J. Bokor, and G. Szederkényi. *Analysis and Control of Nonlinear Process Systems*. Springer, 2004.
- W. G. Hunter and A. M. Reiner. Designs for discriminating between two rival models. *Technometrics*, 7(3):307–323, 1965.
- P. Joy, H. Djelassi, A. Mhamdi, et al. Optimization-based global structural identifiability. *Comp Chem Eng*, 128:417–420, 2019.
- K. J. Keesman and E. Walter. Optimal input design for model discrimination using Pontryagin’s maximum principle: Application to kinetic model structures. *Automatica*, 50:1535–1538, 2014.
- J. Ko, D. J. Klein, D. Fox, et al. Gaussian processes and reinforcement learning for identification and control of an autonomous blimp. In *ICRA*, pages 742–747, 2007.
- D. J. MacKay. *Information theory, inference, and learning algorithms*. Cambridge University Press, 2003.
- D. J. C. MacKay. Information-based objective functions for active data selection. *Neural Comput*, 4:590–604, 1992.
- J. L. Martínez, L. Liu, D. Petranovic, et al. Pharmaceutical protein production by yeast: towards production of human blood proteins by microbial fermentation. *Curr Opin Biotechnol*, 23(6):965–971, 2012.
- A. Mesbah, S. Streif, R. Findeisen, et al. Active fault detection for nonlinear systems with probabilistic uncertainties. In *IFAC 19*, pages 7079–7084, 2014a.
- A. Mesbah, S. Streif, R. Findeisen, et al. Stochastic nonlinear model predictive control with probabilistic constraints. In *ACC*, pages 2413–2419, 2014b.
- C. Michalik, M. Stuckert, and W. Marquardt. Optimal experimental design for discriminating numerous model candidates: The AWDC criterion. *Ind Eng Chem Res*, 49:913–919, 2010.
- U. Naumann. *The art of Differentiating Computer Programs: An Introduction to Algorithmic Differentiation*. SIAM, 2012.
- S. Olofsson, M. P. Deisenroth, and R. Misener. Design of experiments for model discrimination hybridising analytical and data-driven approaches. In *ICML 35*, pages 3908–3917, 2018.
- S. Olofsson, L. Hebing, S. Niefenführ, et al. GPdoemd: A Python package for design of experiments for model discrimination. *Comp Chem Eng*, 125:54–70, 2019.
- B. K. Pagnoncelli, S. Ahmed, and A. Shapiro. Sample average approximation method for chance constrained programming: Theory and applications. *J Optim Theory Appl*, 142(2):399–416, 2009.
- J. A. Paulson, M. Martin-Casas, and A. Mesbah. Optimal Bayesian experiment design for nonlinear dynamic systems with chance constraints. *J Process Control*, 77:155–171, 2019.
- A. Prékopa. *Stochastic Programming*. Springer Netherlands, 1995.
- J. Quiñero-Candela, A. Girard, J. Larsen, et al. Propagation of uncertainty in Bayesian kernel models - application to multiple-step ahead forecasting. In *IEEE ICASSP*, pages 701–704, 2003.
- C. E. Rasmussen and C. K. I. Williams. *Gaussian processes for machine learning*. MIT Press, 2006.
- E. G. Ryan, C. C. Drovandi, J. M. McGree, et al. A review of modern computational algorithms for Bayesian optimal design. *Int Stat Rev*, 84:128–154, 2016.
- S. Sæmundsson, A. Terenin, K. Hofmann, et al. Variational integrator networks for physically meaningful embeddings. In *AISTATS*, 2020.
- H. Salimbeni and M. P. Deisenroth. Doubly stochastic variational inference for deep Gaussian processes. In *NIPS 30*, pages 4588–4599, 2017.
- E. S. Schultz, R. Hannemann-Tamás, and A. Mitsos. Guaranteed satisfaction of inequality state constraints in PDE-constrained optimization. *Automatica*, page 108653, 2019.
- D. Skanda and D. Lebedz. An optimal experimental design approach to model discrimination in dynamic biochemical systems. *Bioinformatics*, 26(7):939–945, 2010.

-
- D. Skanda and D. Lebiedz. A robust optimization approach to experimental design for model discrimination of dynamical systems. *Math Program*, 141:405–433, 2013.
- J. Steensels, T. Snoek, E. Meersman, et al. Improving industrial yeast strains: exploiting natural and artificial diversity. *FEMS Microbiol Rev*, 38(5):947–995, 2014.
- S. Streif, F. Petzke, A. Mesbah, et al. Optimal experimental design for probabilistic model discrimination using polynomial chaos. In *IFAC 19*, pages 4103–4109, 2014.
- N. Wahlström, T. B. Schön, and M. P. Deisenroth. Learning deep dynamical models from image pixels. In *SYSID 17*, pages 1059–1064, 2015.
- O. Walz, H. Djelassi, and A. Mitsos. Optimal experimental design for optimal process design: A trilevel optimization formulation. *AIChE J*, 66(1):e16788, 2020.

A The Bania (2019) Case Study

The Bania (2019) case study considers three rival, linear continuous-time models \mathcal{M}_i , $i \in \{1, 2, 3\}$, of the form

$$\mathcal{M}_i : \begin{cases} \left. \frac{dx}{dt} \right|_t = \mathbf{A}_i x(t) + \mathbf{B}_i u(t) + \mathbf{C}_i w(t), \\ y_k = [1, 0, \dots, 0] x(t_k) + 0.05 \cdot v_k, \end{cases}$$

where $x(t)$ denotes the state at time t , $u(t)$ denotes the control input and w is the process noise given by a Wiener process with variance 1. Measurements y_k are taken at discrete time points t_k , $k = 1, \dots, T$ with Gaussian-distributed measurement noise $v_k \sim \mathcal{N}(0, 1)$. The matrices \mathbf{A}_i , \mathbf{B}_i and \mathbf{C}_i are defined as

$$\begin{aligned} \mathcal{M}_1 : \quad & \mathbf{A}_1 = -1, \quad \mathbf{B}_1 = 1, \quad \mathbf{C}_1 = 0.05, \\ \mathcal{M}_2 : \quad & \mathbf{A}_2 = \begin{bmatrix} 0 & 1 \\ -3 & -2.5 \end{bmatrix}, \quad \mathbf{B}_2 = \begin{bmatrix} 0 \\ 3 \end{bmatrix}, \quad \mathbf{C}_2 = \begin{bmatrix} 0 \\ 0.05 \end{bmatrix}, \\ \mathcal{M}_3 : \quad & \mathbf{A}_3 = \begin{bmatrix} 0 & 1 & 0 \\ -3 & -3.5 & 1 \\ 0 & 0 & -10 \end{bmatrix}, \quad \mathbf{B}_3 = \begin{bmatrix} 0 \\ 0 \\ 30 \end{bmatrix}, \quad \mathbf{C}_3 = \begin{bmatrix} 0 \\ 0 \\ 0.05 \end{bmatrix}. \end{aligned}$$

The initial latent state is $\vec{x}_0^{(i)} = [0, \dots, 0]^\top$.

B Analytical Design of Dynamic Experiments

Extensions of the analytical methods exist for design of dynamic experiments. Espie and Macchietto (1989) consider discrimination between multiple analytic continuous-time models and formulate an optimal control problem. Espie and Macchietto (1989) compare the results of using optimal constant control inputs *versus* an optimal dynamic control input. Chen and Asprey (2003) also consider continuous-time models and use a Laplace approximation for the model parameter covariance and linear propagation of the Gaussian model parameter uncertainty to approximate the marginal predictive distributions.

Skanda and Lebiez (2010) assume Gaussian measurement noise to derive an expression for the Kullback-Leibler (KL) divergence between the predictive distributions of two rival models (with the same number of states). They include the measurement time points $\mathcal{T}_{\text{meas}}$ as variables in the optimisation problem, together with the initial state $x(0) = \vec{x}_0$ and control inputs $\vec{u}_{0:T-1}$. The control inputs Skanda and Lebiez (2010) consider are additive perturbations to the state, and they assume the states cannot be measured and perturbed in the same time step. Skanda and Lebiez (2013) extend the setup of Skanda and Lebiez (2010) by considering model parameter uncertainty. They propose a robust optimisation formulation

$$\arg \max_{\substack{\mathcal{T}_{\text{meas}} \\ \vec{x}_0 \in \mathcal{X} \\ \vec{u}_{0:T-1} \in \mathcal{U}}} \min_{\substack{i, j \in \{1, \dots, M\} \\ i \neq j}} \min_{\substack{\vec{\theta}_i \in \vec{\Theta}_i \\ \vec{\theta}_j \in \vec{\Theta}_j}} \sum_{k \in \mathcal{T}_{\text{meas}}} \text{KL} \left[p(\vec{y}_k | \vec{\theta}_i) \parallel p(\vec{y}_k | \vec{\theta}_j) \right]$$

subject to constraints, with model parameter spaces $\vec{\Theta}_i$ and $\vec{\Theta}_j$ and $p(\vec{y}_k | \vec{\theta}_i)$ denoting the predictive distribution at time step k given model i with parameter values $\vec{\theta}_i$.

None of Espie and Macchietto (1989), Chen and Asprey (2003), or Skanda and Lebiez (2010, 2013) consider process noise or uncertainty in the initial state $x(0) = \vec{x}_0$ or control signal $u(t)$. Nor do any of them, when solving the optimisation problem subject to dependent variable constraints on the observed states $\vec{z}_{1:T}$, account for the uncertainty in the observed states $\vec{z}_{1:T}$ predictions.

Cheong and Manchester (2014) consider non-parametric linear discrete-time systems with process noise (but no separate measurement noise) and uncertainty in the initial states \vec{x}_0 . For optimising the control signal they consider design criteria based on the pairwise difference

in models' score in the χ^2 goodness-of-fit test. Though Cheong and Manchester (2014) consider dependent variable constraints in the observed states $\bar{z}_{1:T}$, they do not account for the uncertainty in the observed states $\bar{z}_{1:T}$ predictions.

Streif et al. (2014) and Mesbah et al. (2014a) look at cases of two rival non-linear models \mathcal{M}_1 and \mathcal{M}_2 with multiplicative measurement noise

$$\mathcal{M}_i : \begin{cases} \left. \frac{dx(t)}{dt} \right|_t = f_i(x(t), u(t), \vec{\theta}_i), \\ z(t) = g_i(x(t), u(t), \vec{\theta}_i), \\ \vec{y}_k = \text{diag}(\vec{1} + \vec{w}_k) \vec{z}_k \end{cases}$$

where f_i and g_i , $i \in \{1, 2\}$, are polynomial functions. They consider uncertainty in the initial states and model parameters using polynomial chaos expansions, from which they compute higher moments of the predictive distributions—"a computationally formidable task" according to Streif et al. (2014). They discretise the control signal and solve the design problem by minimising the norm of the control signal such that the divergence between the predictive distributions is greater than or equal to some threshold value. The divergence can be computed using the predictive distributions' higher moments (Streif et al., 2014) or through Markov Chain Monte Carlo integration (Mesbah et al., 2014a).

Keesman and Walter (2014) look at continuous-time models of the kind $\frac{d}{dt}y(t) = f(y(t)) + bu(t)$. They define the Hamiltonian and from this derive an optimal control law in closed form for two rival models. This requires gradient information of *at least* the first order. They do not account for parametric uncertainty, process noise or measurement noise.

Bania (2019) consider non-parametric linear discrete-time models with process and measurement noise. By looking at the mutual information between choice of model and observed output, they derive an optimisation formulation based on minimising the probability of selecting the wrong model. They mention how to extend their approach to non-linear models.

C Continuous-Time State Space Models

The continuous-time state space models is described by

$$\mathcal{M} : \begin{cases} \left. \frac{dx}{dt} \right|_t = f_i(x(t), u(t), \vec{\theta}) + w(t), \\ x(t_0) \equiv \vec{x}_0, \\ z(t) = \mathbf{H}x(t), \\ \vec{y}_k = z(t_k) + \vec{v}_k, \end{cases}$$

with state $x(t)$, control input $u(t)$, process noise distribution $w(t) \sim \mathcal{N}(\vec{0}, \vec{\Sigma}_x)$. The control input $u(t_k)$ may be a continuous function of the time t , but we will assume it is piece-wise constant. Model \mathcal{M} 's state prediction at time step k is given by

$$\vec{x}_k = \vec{x}_{k-1} + \int_{t_{k-1}}^{t_k} f(x(t), \vec{u}_{k-1}, \vec{\theta}) dt + \vec{w}_k$$

where $w(t) \sim \mathcal{N}(\vec{0}, (t_k - t_{k-1})\vec{\Sigma}_x)$.

Let $\tilde{x}(t)$ denote the continuous concatenated state, control input and model parameters $\tilde{x}(t) = [x(t)^\top, u(t)^\top, \vec{\theta}^\top]^\top$, with Gaussian distribution $\tilde{x}(t) \sim \mathcal{N}(\tilde{\mu}(t), \tilde{\Sigma}(t))$, and let $\tilde{\mu}_f$ denote the concatenated transition function

$$\tilde{\mu}_f(t) = [\mu_f(\tilde{\mu}(t))^\top, \vec{0}, \vec{0}]^\top, \quad \tilde{\mu}_f(t) \in \mathbb{R}^{D_x + D_u + D_\theta}.$$

We find the state prediction $\vec{x}_k \sim \mathcal{N}(\vec{\mu}_k, \vec{\Sigma}_k)$ at time step k by extracting the corresponding elements from $\tilde{\mu}(t_k)$ and $\tilde{\Sigma}(t)$ (see (8)) which we compute by solving the following system of

ordinary differential equations

$$\begin{cases} \left. \frac{d\tilde{\mu}}{dt} \right|_t = \tilde{\mu}_f(t), \\ \left. \frac{d\tilde{\Sigma}}{dt} \right|_t = \nabla_{\tilde{\mu}(t)} \tilde{\mu}_f \tilde{\Sigma}(t) + \tilde{\Sigma}(t) (\nabla_{\tilde{\mu}(t)} \tilde{\mu}_f)^\top + \text{diag}(\Sigma_f(\tilde{\mu}(t)) + \tilde{\Sigma}_x, \vec{0}, \vec{0}), \\ \tilde{\mu}(t_{k-1}) \equiv \tilde{\mu}_{k-1}, \\ \tilde{\Sigma}(t_{k-1}) \equiv \tilde{\Sigma}_{k-1}. \end{cases}$$

Derivatives of $\tilde{\mu}_{k+1}$ and $\tilde{\Sigma}_{k+1}$ with respect to $\tilde{\mu}_k$, $\tilde{\Sigma}_k$ and \hat{u}_k are calculated by integrating over the chain rule, and require second-order derivative information of f or the GP prediction.

For continuous-time models we may wish to optimise the measurement time instances $\mathcal{T}_{\text{meas}}$. In this case a minimum amount of time between measurements need to be enforced during optimisation. Let the absolute difference in time between two measurement time points t_k and $t_{k'}$ be lower-bounded by $\Delta_t \geq 0$

$$|t_k - t_{k'}| \geq \Delta_t, \quad \forall t_k, t_{k'} \in \mathcal{T}_{\text{meas}}. \quad (11)$$

This constraint is non-convex. To simplify the problem formulation, we introduce additional constraints to maintain a fixed order of the measurement time points, and reformulate (11) in convex form as

$$\forall t_k, t_{k'} \in \mathcal{T}_{\text{meas}} : \begin{cases} t_k - t_{k'} - \Delta_t \geq 0, & k \geq k', \\ t_{k'} - t_k - \Delta_t \geq 0, & k < k'. \end{cases}$$

using the constraints format in (5).

D Discrete-Time Model with Δ -Transition

The discrete-time state space model with a Δ -transition is described by

$$\mathcal{M} : \begin{cases} \vec{x}_{k+1} = \vec{x}_k + f(\vec{x}_k, \vec{u}_k, \vec{\theta}) + \vec{w}_k, \\ \vec{z}_k = \mathbf{H}\vec{x}_k, \\ \vec{y}_k = \vec{z}_k + \vec{v}_k, \end{cases}$$

with process noise $\vec{w}_k \sim \mathcal{N}(\vec{0}, \tilde{\Sigma}_x)$. The discrete-time model with a Δ -transition follows from an Euler discretisation of continuous-time dynamics (Atkinson *et al.*, 2009, Ch. 2). Using a first-order Taylor expansion of $\mu_f(\vec{x})$ around $\tilde{x}_{k-1} = \tilde{\mu}_{k-1}$, the mean and variance of the state at time step $k \geq 1$ in (7a) are approximately given by

$$\begin{aligned} \tilde{\mu}_k &\approx \tilde{\mu}_{k-1} + \mu_f(\tilde{\mu}_{k-1}), \\ \tilde{\Sigma}_k &\approx \nabla_{\tilde{x}_{k-1}} \tilde{\mu}_k \tilde{\Sigma}_{k-1} \left(\nabla_{\tilde{x}_{k-1}} \tilde{\mu}_k \right)^\top + \tilde{\Sigma}_x + \Sigma_f(\tilde{\mu}_k), \\ \text{cov}(\vec{x}_k, \vec{\theta}) &\approx \text{cov}(\vec{x}_{k-1}, \vec{\theta}) + \nabla_{\vec{\theta}} \tilde{\mu}_k \text{cov}(\vec{x}_{k-1}, \vec{\theta})^\top + \nabla_{\vec{\theta}} \tilde{\mu}_k \tilde{\Sigma}_{\theta}. \end{aligned}$$

Note that $\nabla_{\tilde{x}_{k-1}} \tilde{\mu}_k = \mathbf{I} + \nabla_{\tilde{x}_{k-1}} \mu_f$ with the Δ -transition model, and that $\nabla_{\tilde{x}_{k-1}} \tilde{\mu}_k \in \mathbb{R}^{D_x \times (D_x + D_u + D_\theta)}$. Derivatives of $\tilde{\mu}_k$ and $\tilde{\Sigma}_k$ with respect to $\tilde{\mu}_{k-1}$, $\tilde{\Sigma}_{k-1}$ and \hat{u}_{k-1} are calculated following the standard rules of matrix calculus, and requires second-order derivative information of f or the GP prediction.

It is common in GP regression to use zero-mean GP priors ($m_{(d)}(\cdot) \equiv 0$) to simplify calculations. The zero-mean prior is suitable for the Δ -transition state space model formulation (Ko *et al.*, 2007; Deisenroth and Rasmussen, 2011).

E Design of Experiments Algorithm

Input : Data points \mathbf{U} (controls) and \mathbf{Y} (measurements);
 Model candidates $\mathcal{M}_1, \dots, \mathcal{M}_M$;
 Feasible state spaces $\mathcal{X}_1, \dots, \mathcal{X}_M$ and control space \mathcal{U} ;
 Number of training data points N_1, \dots, N_M for GP surrogate models;
 Experiment budget j_{\max} (max no. of additional experiments);
 Model relevance threshold χ_{lower}^2 , such as 1E-3;

Output: Selected model \mathcal{M}^* with parameter estimate $\hat{\theta}^* \sim \mathcal{N}(\hat{\theta}^*, \hat{\Sigma}_{\theta}^*)$;

```

1 for  $j \leftarrow 1$  to  $j_{\max}$  do
2   for  $i \leftarrow 1$  to  $M$  do
3     Available data  $\mathbf{U}$  and  $\mathbf{Y}$  used for parameter estimation;
4      $\tilde{\theta}_i \leftarrow$  Model  $\mathcal{M}_i$ 's maximum a posteriori parameter estimate;
5     if model  $\mathcal{M}_i$  is a black box then
6       Construct GP surrogate model training data;
7        $\tilde{\mathbf{X}}_t \leftarrow$  sample  $N_i$  states from  $\mathcal{X}_i$ ;
8        $\tilde{\mathbf{U}}_t \leftarrow$  sample  $N_i$  controls from  $\mathcal{U}$ ;
9        $\tilde{\Theta}_t \leftarrow$  sample  $N_i$  model parameters from  $\mathcal{N}(\tilde{\theta}_i, \epsilon \cdot \mathbf{I})$ ;
10      Initialise  $\tilde{\mathbf{X}}_{t+1} \in \mathbb{R}^{N_i \times D_x}$  as empty array;
11      for  $n \leftarrow 1$  to  $N_i$  do
12         $\tilde{\mathbf{X}}_{t+1,n} \leftarrow f_i(\tilde{\mathbf{X}}_{t,n}, \tilde{\mathbf{U}}_{t,n}, \tilde{\Theta}_{t,n})$ ;
13      end
14      Learn GP surrogate model hyperparameters  $\tilde{\lambda}_i$ ;
15       $\tilde{\lambda}_i \leftarrow \arg \max_{\tilde{\lambda}} p(\tilde{\mathbf{X}}_{t+1} | \tilde{\mathbf{X}}_t, \tilde{\mathbf{U}}_t, \tilde{\Theta}_t, \tilde{\lambda})$ 
16    end
17    Available data  $\mathbf{U}$  and  $\mathbf{Y}$  used for parameter estimation;
18     $\tilde{\Sigma}_{\theta,i} \leftarrow$  Laplace approximation of model parameter covariance;
19    Available data  $\mathbf{U}$  and  $\mathbf{Y}$  used for model relevance check;
20     $\chi_i^2 \leftarrow$  Model  $\mathcal{M}_i$ 's  $\chi^2$  score;
21  end
22  Select models with sufficiently high  $\chi^2$  score;
23   $\mathcal{M}_{\{\}} \leftarrow \{\mathcal{M}_i \text{ if } \chi_i^2 \geq \chi_{\text{lower}}^2\}$ ;
24  if  $|\mathcal{M}_{\{\}}| \leq 1$  then
25    Best model found, or all models discarded;
26    BREAK;
27  else
28    Generate additional experimental data;
29     $\tilde{u}_j^* \leftarrow$  solution to design of experiments problem (5) for models  $\mathcal{M}_{\{\}}$ ;
30     $\tilde{y}_j \leftarrow$  measurements from running experiment with controls  $\tilde{u}_j^*$ ;
31     $\mathbf{U} \leftarrow \text{concatenate}(\mathbf{U}, \tilde{u}_j^*)$ ;
32     $\mathbf{Y} \leftarrow \text{concatenate}(\mathbf{Y}, \tilde{y}_j)$ ;
33  end
34 end
35 if  $|\mathcal{M}_{\{\}}| = 1$  then
36   Success! One model  $\mathcal{M}^*$  remaining;
37 else
38   Inconclusive result! More than one model (or no models) remaining;
39 end

```

Algorithm 1: The design of experiments process.

F Yeast Fermentation Case Study

The yeast fermentation case study is taken from Espie and Macchietto (1989), with constants (for example for true parameter values and noise covariances) taken from Chen and Asprey (2003). There are $D_x = 2$ latent states (biomass and substrate concentration, respectively) and $D_u = 2$ control inputs (feed velocity and feed substrate concentration). We observe both states, hence $D_z = D_y = 2$ and $\mathbf{H}_i = \mathbf{H} = \mathbf{I}$, with $D_{\theta,i} \in \{3, 4\}$ model parameters. For simplicity, we omit the model index and time step index when writing out the models

$$\mathcal{M}_1 : \begin{cases} \frac{dx_1}{dt} = (r - u_1 - \theta_4)x_1, \\ \frac{dx_2}{dt} = -\frac{rx_1}{\theta_3} + u_1(u_2 - x_2), \\ r = \frac{\theta_1 x_2}{\theta_2 + x_2}. \end{cases}$$

$$\mathcal{M}_2 : \begin{cases} \frac{dx_1}{dt} = (r - u_1 - \theta_4)x_1, \\ \frac{dx_2}{dt} = -\frac{rx_1}{\theta_3} + u_1(u_2 - x_2), \\ r = \frac{\theta_1 x_2}{\theta_2 x_1 + x_2}. \end{cases}$$

$$\mathcal{M}_3 : \begin{cases} \frac{dx_1}{dt} = (r - u_1 - \theta_3)x_1, \\ \frac{dx_2}{dt} = -\frac{rx_1}{\theta_2} + u_1(u_2 - x_2), \\ r = \theta_1 x_2. \end{cases}$$

$$\mathcal{M}_4 : \begin{cases} \frac{dx_1}{dt} = (r - u_1)x_1, \\ \frac{dx_2}{dt} = -\frac{rx_1}{\theta_3} + u_1(u_2 - x_2), \\ r = \frac{\theta_1 x_2}{\theta_2 + x_2}. \end{cases}$$

Data is generated from \mathcal{M}_1 with parameters $\vec{\theta} = [0.25, 0.25, 0.88, 0.09]$ (Chen and Asprey, 2003). The measurement noise covariance is assumed known and given by

$$\vec{\Sigma}_y = \begin{bmatrix} 0.06 & -0.01 \\ -0.01 & 0.04 \end{bmatrix},$$

and there is no process noise, hence $\vec{\Sigma}_x \equiv \vec{0}$. We start without any experimental data and initial model parameter estimates $\theta_{i,d} = 0.5$ and covariance $\vec{\Sigma}_{\theta,i} = 0.05 \cdot \mathbf{I}$ for all models \mathcal{M}_i and $d \in \{1, \dots, D_{\theta,i}\}$. The reason for this is the difficulty in finding initial experimental conditions that do not immediately render one or more models obviously inadequate. The initial states are given by $x_1 = 1$ and $x_2 = 0.01$, with initial latent state covariance $\vec{\Sigma}_0 = \text{diag}(10^{-3}, 10^{-6})$. The controls have bounds $u_1 \in [0.05, 0.2]$ and $u_2 \in [5, 35]$. We let the control inputs have covariance given by $\vec{\Sigma}_u = \text{diag}(10^{-6}, 10^{-3})$. We simulate 72 hours of fermentation, with measurements and changes in control signal every 1.5 hours.